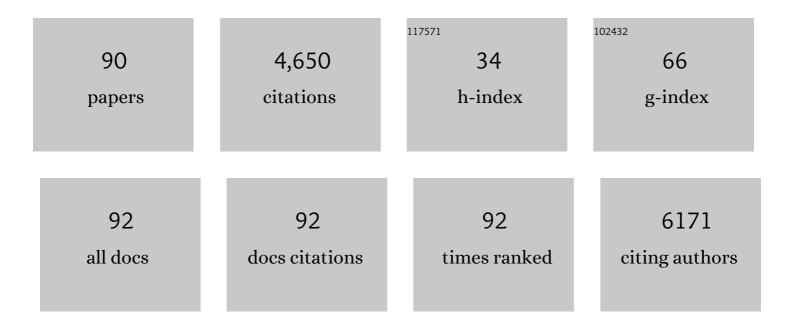
List of Publications by Year in descending order

Source: https://exaly.com/author-pdf/5427261/publications.pdf Version: 2024-02-01



#	Article	IF	CITATIONS
1	Introduction of amino groups into acid-resistant MOFs for enhanced U(<scp>vi</scp>) sorption. Journal of Materials Chemistry A, 2015, 3, 525-534.	5.2	378
2	Sulfur-anchoring synthesis of platinum intermetallic nanoparticle catalysts for fuel cells. Science, 2021, 374, 459-464.	6.0	343
3	Reversing the charge transfer between platinum and sulfur-doped carbon support for electrocatalytic hydrogen evolution. Nature Communications, 2019, 10, 4977.	5.8	243
4	SiO ₂ -protected shell mediated templating synthesis of Fe–N-doped carbon nanofibers and their enhanced oxygen reduction reaction performance. Energy and Environmental Science, 2018, 11, 2208-2215.	15.6	196
5	A sulfur-tethering synthesis strategy toward high-loading atomically dispersed noble metal catalysts. Science Advances, 2019, 5, eaax6322.	4.7	177
6	Identification of Catalytic Sites for Oxygen Reduction in Metal/Nitrogenâ€Doped Carbons with Encapsulated Metal Nanoparticles. Angewandte Chemie - International Edition, 2020, 59, 1627-1633.	7.2	176
7	One-pot synthesis of porous 1T-phase MoS2 integrated with single-atom Cu doping for enhancing electrocatalytic hydrogen evolution reaction. Applied Catalysis B: Environmental, 2019, 251, 87-93.	10.8	160
8	Identification of Catalytic Sites for Oxygen Reduction in Metal/Nitrogenâ€Đoped Carbons with Encapsulated Metal Nanoparticles. Angewandte Chemie, 2020, 132, 1644-1650.	1.6	138
9	Aqueous Electrolytes with Hydrophobic Organic Cosolvents for Stabilizing Zinc Metal Anodes. ACS Nano, 2022, 16, 9667-9678.	7.3	126
10	Precise fabrication of single-atom alloy co-catalyst with optimal charge state for enhanced photocatalysis. National Science Review, 2021, 8, nwaa224.	4.6	125
11	Origin of the different phytotoxicity and biotransformation of cerium and lanthanum oxide nanoparticles in cucumber. Nanotoxicology, 2015, 9, 262-270.	1.6	123
12	Introduction of Bifunctional Groups into Mesoporous Silica for Enhancing Uptake of Thorium(IV) from Aqueous Solution. ACS Applied Materials & Interfaces, 2014, 6, 4786-4796.	4.0	113
13	Photoelectric conversion on Earth's surface via widespread Fe- and Mn-mineral coatings. Proceedings of the United States of America, 2019, 116, 9741-9746.	3.3	111
14	Superconductivity in Pristine <mml:math <br="" xmlns:mml="http://www.w3.org/1998/Math/MathML">display="inline"><mml:mrow><mml:mn>2</mml:mn><mml:msub><mml:mrow><mml:mi>H</mml:mi> at Ultrahigh Pressure. Physical Review Letters, 2018, 120, 037002.</mml:mrow></mml:msub></mml:mrow></mml:math>	rovæ.9 mml	:m 10% > <mm< td=""></mm<>
15	Sulfur stabilizing metal nanoclusters on carbon at high temperatures. Nature Communications, 2021, 12, 3135.	5.8	104
16	Correlating interfacial octahedral rotations with magnetism in (LaMnO3+δ)N/(SrTiO3)N superlattices. Nature Communications, 2014, 5, 4283.	5.8	103
17	Activation of subnanometric Pt on Cu-modified CeO2 via redox-coupled atomic layer deposition for CO oxidation. Nature Communications, 2020, 11, 4240.	5.8	101
18	<i>Operando</i> X-ray spectroscopy visualizing the chameleon-like structural reconstruction on an oxygen evolution electrocatalyst. Energy and Environmental Science, 2021, 14, 906-915.	15.6	93

#	Article	IF	CITATIONS
19	Activated-carbon-supported K–Co–Mo catalysts for synthesis of higher alcohols from syngas. Catalysis Science and Technology, 2015, 5, 2925-2934.	2.1	90
20	Enhanced removal of roxarsone by Fe ₃ O ₄ @3D graphene nanocomposites: synergistic adsorption and mechanism. Environmental Science: Nano, 2017, 4, 2134-2143.	2.2	89
21	Transformation of ceria nanoparticles in cucumber plants is influenced by phosphate. Environmental Pollution, 2015, 198, 8-14.	3.7	84
22	The double influence mechanism of pH on arsenic removal by nano zero valent iron: electrostatic interactions and the corrosion of Fe ⁰ . Environmental Science: Nano, 2017, 4, 1544-1552.	2.2	78
23	Highly Selective Oxidation of Methane into Methanol over Cu-Promoted Monomeric Fe/ZSM-5. ACS Catalysis, 2021, 11, 6684-6691.	5.5	73
24	Ternary composite oxide catalysts CuO/Co3O4–CeO2 with wide temperature-window for the preferential oxidation of CO in H2-rich stream. Chemical Engineering Journal, 2013, 234, 88-98.	6.6	67
25	Oxideâ€Nanotrapâ€Anchored Platinum Nanoparticles with High Activity and Sintering Resistance by Areaâ€Selective Atomic Layer Deposition. Angewandte Chemie - International Edition, 2017, 56, 1648-1652.	7.2	65
26	Nanofence Stabilized Platinum Nanoparticles Catalyst via Facet‧elective Atomic Layer Deposition. Small, 2017, 13, 1700648.	5.2	61
27	Direct Synthesis of Stable 1Tâ€MoS ₂ Doped with Ni Single Atoms for Water Splitting in Alkaline Media. Small, 2022, 18, e2107238.	5.2	58
28	Selective Passivation of Pt Nanoparticles with Enhanced Sintering Resistance and Activity toward CO Oxidation via Atomic Layer Deposition. ACS Applied Nano Materials, 2018, 1, 522-530.	2.4	47
29	Architecting Freestanding Sulfur Cathodes for Superior Roomâ€Temperature Na–S Batteries. Advanced Functional Materials, 2021, 31, 2102280.	7.8	46
30	Fabrication of a Singleâ€Atom Platinum Catalyst for the Hydrogen Evolution Reaction: A New Protocol by Utilization of H _{<i>x</i>} MoO _{3â^'<i>x</i>} with Plasmon Resonance. ChemCatChem, 2018, 10, 946-950.	1.8	43
31	Zeoliteâ€Tailored Active Site Proximity for the Efficient Production of Pentanoic Biofuels. Angewandte Chemie - International Edition, 2021, 60, 23713-23721.	7.2	43
32	Nickel catalyst with atomically-thin meshed cobalt coating for improved durability in dry reforming of methane. Journal of Catalysis, 2019, 373, 351-360.	3.1	42
33	Understanding the Mesoscale Degradation in Nickel-Rich Cathode Materials through Machine-Learning-Revealed Strain–Redox Decoupling. ACS Energy Letters, 2021, 6, 687-693.	8.8	42
34	Decreasing the Overpotential of Aprotic Li O ₂ Batteries with the Inâ€Plane Alloy Structure in Ultrathin 2D Ruâ€Based Nanosheets. Advanced Functional Materials, 2022, 32, .	7.8	39
35	Hierarchically porous carbons as supports for fuel cell electrocatalysts with atomically dispersed Fe–N _x moieties. Chemical Science, 2019, 10, 8236-8240.	3.7	34
36	Improved NO–CO reactivity of highly dispersed Pt particles on CeO ₂ nanorod catalysts prepared by atomic layer deposition. Catalysis Science and Technology, 2019, 9, 2664-2672.	2.1	34

#	Article	IF	CITATIONS
37	Bifunctional CO oxidation over Mn-mullite anchored Pt sub-nanoclusters <i>via</i> atomic layer deposition. Chemical Science, 2018, 9, 2469-2473.	3.7	33
38	Highly efficient and selective electrocatalytic hydrogen peroxide production on Co-O-C active centers on graphene oxide. Communications Chemistry, 2022, 5, .	2.0	33
39	Porous CoP/C@MCNTs hybrid composite derived from metal–organic frameworks for high-performance lithium-ion batteries. Journal of Materials Science, 2019, 54, 3273-3283.	1.7	29
40	Iron Isotope Effect and Local Lattice Dynamics in the (Ba, K)Fe2As2 Superconductor Studied by Temperature-Dependent EXAFS. Scientific Reports, 2013, 3, .	1.6	27
41	High Co-doping promotes the transition of birnessite layer symmetry from orthogonal to hexagonal. Chemical Geology, 2015, 410, 12-20.	1.4	27
42	Oxideâ€Nanotrapâ€Anchored Platinum Nanoparticles with High Activity and Sintering Resistance by Areaâ€Selective Atomic Layer Deposition. Angewandte Chemie, 2017, 129, 1670-1674.	1.6	27
43	Rational design of hierarchical FeSe ₂ encapsulated with bifunctional carbon cuboids as an advanced anode for sodium-ion batteries. Nanoscale, 2020, 12, 22210-22216.	2.8	26
44	Atomic Structural Evolution of Single‣ayer Pt Clusters as Efficient Electrocatalysts. Small, 2021, 17, e2100732.	5.2	26
45	Effects of Mn average oxidation state on the oxidation behaviors of As(III) and Cr(III) by vernadite. Applied Geochemistry, 2018, 94, 35-45.	1.4	23
46	Cationâ~'Ï€ Interactions with Coexisting Heavy Metals Enhanced the Uptake and Accumulation of Polycyclic Aromatic Hydrocarbons in Spinach. Environmental Science & Technology, 2020, 54, 7261-7270.	4.6	22
47	Sol–gel synthesis and electrochemical properties of c-axis oriented LiCoO ₂ for lithium-ion batteries. RSC Advances, 2015, 5, 51483-51488.	1.7	21
48	Highly dispersed Pt studded on CoO _x nanoclusters for CO preferential oxidation in H ₂ . Journal of Materials Chemistry A, 2020, 8, 10180-10187.	5.2	21
49	Sub-2 nm Ir Nanoclusters Immobilized on Mesoporous Nitrogen-Doped Carbons as Efficient Catalysts for Selective Hydrogenation. ACS Applied Nano Materials, 2019, 2, 6546-6553.	2.4	20
50	Switching Co/N/C Catalysts for Heterogeneous Catalysis and Electrocatalysis by Controllable Pyrolysis of Cobalt Porphyrin. IScience, 2019, 15, 282-290.	1.9	20
51	The chemical speciation, spatial distribution and toxicity of mercury from Tibetan medicine Zuotai,β-HgS and HgCl2 in mouse kidney. Journal of Trace Elements in Medicine and Biology, 2018, 45, 104-113.	1.5	19
52	Mechanisms of Synergistic Removal of Low Concentration As(V) by nZVI@Mg(OH) ₂ Nanocomposite. Journal of Physical Chemistry C, 2017, 121, 21411-21419.	1.5	18
53	A library of carbon-supported ultrasmall bimetallic nanoparticles. Nano Research, 2020, 13, 2735-2740.	5.8	18
54	Pressure-Induced Valence Change and Semiconductor–Metal Transition in PbCrO ₃ . Journal of Physical Chemistry C, 2014, 118, 23274-23278.	1.5	17

#	Article	IF	CITATIONS
55	Synthesis of carbon-supported sub-2 nanometer bimetallic catalysts by strong metal–sulfur interaction. Chemical Science, 2020, 11, 7933-7939.	3.7	17
56	Application of Xâ€Ray Absorption Spectroscopy in Electrocatalytic Water Splitting and CO ₂ Reduction. Small Science, 2021, 1, 2100023.	5.8	16
57	Influence of phosphate on phytotoxicity of ceria nanoparticles in an agar medium. Environmental Pollution, 2017, 224, 392-399.	3.7	15
58	Cu(<scp>ii</scp>) sorption by biogenic birnessite produced by <i>Pseudomonas putida</i> strain MnB1: structural differences from abiotic birnessite and its environmental implications. CrystEngComm, 2018, 20, 1361-1374.	1.3	15
59	Magnetic Particles Unintentionally Emitted from Anthropogenic Sources: Iron and Steel Plants. Environmental Science and Technology Letters, 2021, 8, 295-300.	3.9	15
60	Structural characteristic correlated to the electronic band gap in <mml:math xmlns:mml="http://www.w3.org/1998/Math/MathML"><mml:mrow><mml:mi>Mo</mml:mi><mml:msub><mml:m mathvariant="normal">S<mml:mn>2</mml:mn></mml:m </mml:msub></mml:mrow>. Physical Review B, 2016, 94, .</mml:math 	¹ⁱ 1.1	14
61	A new type of noncovalent surface–π stacking interaction occurring on peroxide-modified titania nanosheets driven by vertical π-state polarization. Chemical Science, 2021, 12, 4411-4417.	3.7	13
62	Confocal depth-resolved fluorescence micro-X-ray absorption spectroscopy for the study of cultural heritage materials: a new mobile endstation at the Beijing Synchrotron Radiation Facility. Journal of Synchrotron Radiation, 2017, 24, 1000-1005.	1.0	11
63	Zeoliteâ€Tailored Active Site Proximity for the Efficient Production of Pentanoic Biofuels. Angewandte Chemie, 2021, 133, 23906-23914.	1.6	10
64	Study of OSEM with different subsets in grating-based X-ray differential phase-contrast imaging. Analytical and Bioanalytical Chemistry, 2011, 401, 837-844.	1.9	9
65	[MW ₁₂ O ₄₄] clusters: unprecedented central heteroatoms atomically dispersed in the eight coordination state bridging the 1 : 12 polyoxometalate family of Keggin and Silverton. Nanoscale, 2019, 11, 22270-22276.	2.8	9
66	Microporous Sulfur-Doped Carbon Atoms as Supports for Sintering-Resistant Platinum Nanocluster Catalysts. ACS Applied Nano Materials, 2021, 4, 9489-9496.	2.4	9
67	Influences of the Amorphous Phase on Local Structures and Properties of Ferroelectric Thin Films. Ferroelectrics, 2013, 453, 149-155.	0.3	8
68	In-situ EXAFS study on the thermal decomposition of TiH ₂ . Chinese Physics C, 2014, 38, 038001.	1.5	8
69	Time-resolved XAFS measurement using quick-scanning techniques at BSRF. Journal of Synchrotron Radiation, 2017, 24, 674-678.	1.0	8
70	A metal-catalyzed thermal polymerization strategy toward atomically dispersed catalysts. Chemical Communications, 2019, 55, 11579-11582.	2.2	8
71	Prediction of topological nontrivial semimetals and pressure-induced Lifshitz transition in 1T′-MoS ₂ layered bulk polytypes. Nanoscale, 2020, 12, 22710-22717.	2.8	8
72	Optimal azimuthal orientation for Si(111) double-crystal monochromators to achieve the least amount of glitches in the hard X-ray region. Journal of Synchrotron Radiation, 2015, 22, 1147-1150.	1.0	7

#	Article	IF	CITATIONS
73	Pressure induced transformation and subsequent amorphization of monoclinic Nb ₂ O ₅ and its effect on optical properties. Journal of Physics Condensed Matter, 2019, 31, 105401.	0.7	7
74	High-Temperature Synthesis of Small-Sized Pt/Nb Alloy Catalysts on Carbon Supports for Hydrothermal Reactions. Inorganic Chemistry, 2020, 59, 15953-15961.	1.9	7
75	Experimental and Theoretical Insights into Enhanced Hydrogen Evolution over PtCo Nanoalloys Anchored on a Nitrogen-Doped Carbon Matrix. Journal of Physical Chemistry Letters, 2022, 13, 5195-5203.	2.1	7
76	Discerning lattice and electronic structures in under- and over-doped multiferroic Aurivillius films. Journal of Applied Physics, 2017, 121, 114107.	1.1	6
77	Solvent coordination engineering for high-quality hybrid organic-inorganic perovskite films. Journal of Materials Science, 2021, 56, 9903-9913.	1.7	6
78	The measurement of differential EXAFS modulated by high pressure. Journal of Synchrotron Radiation, 2011, 18, 728-732.	1.0	5
79	Quantum critical point in SmO1â°'xFxFeAs and oxygen vacancy induced by high fluorine dopant. Journal of Synchrotron Radiation, 2011, 18, 723-727.	1.0	5
80	Approach to electrochemical modulating differential extended X-ray absorption fine structure. Journal of Synchrotron Radiation, 2022, 29, 1065-1073.	1.0	5
81	Unraveling the Low-Temperature Redox Behavior of Ultrathin Ceria Nanosheets with Exposed {110} Facets by in Situ XAFS/DRIFTS Utilizing CO as Molecule Probe. Journal of Physical Chemistry C, 2019, 123, 322-333.	1.5	4
82	Surface Ligand Tuning of Coordination Geometry and Pb 6s ² Electronic Pair Stereochemical Activity in MAPbBr ₃ Perovskite Nanoparticles: A Joint Experimental and Theoretical Insight. Journal of Physical Chemistry C, 2022, 126, 7500-7509.	1.5	4
83	Synthesis of Carbon–Metal Oxide Composites as Catalyst Supports by "Cooking Sugar with Salt― ACS Sustainable Chemistry and Engineering, 2022, 10, 731-737.	3.2	3
84	Development of pressure-modulated EXAFS method. Chinese Physics C, 2012, 36, 184-187.	1.5	2
85	A polarization-switch effect of silicon crystals under multiple-beam diffraction geometry. Journal of Applied Crystallography, 2021, 54, 976-981.	1.9	2
86	A new technique to measure the differential XAFS spectrum. Chinese Physics C, 2016, 40, 048001.	1.5	1
87	In situ depth-resolved synchrotron radiation X-ray spectroscopy study of radiation-induced Au deposition. Journal of Synchrotron Radiation, 2019, 26, 1940-1944.	1.0	1
88	Extracting structural information of higher coordination shells by analyzing EXAFS derivative spectrum. Physica Scripta, 2018, 93, 125701.	1.2	0
89	Innenrücktitelbild: Identification of Catalytic Sites for Oxygen Reduction in Metal/Nitrogenâ€Đoped Carbons with Encapsulated Metal Nanoparticles (Angew. Chem. 4/2020). Angewandte Chemie, 2020, 132, 1759-1759.	1.6	0
90	A new mobile grazing-incidence X-ray absorption fine spectroscopy endstation at Beijing Synchrotron Radiation Facility. Radiation Detection Technology and Methods, 0, , .	0.4	0